Kirkuk Journal of Medical Sciences

ORIGINAL ARTICLE

Distribution and Variability of Trabecular Attenuation in the Thoracic Spine on Routine Chest CT

Israa Mohammed Sadiq [1,*] and Saman Anwer Nooruldeen [2]

[1]*Department of Surgery/Radiology, College of Medicine, University of Kirkuk, Kirkuk, Iraq*
[2]*Department of Radiology, Azadi Teaching Hospital, Kirkuk, Iraq*

[*]*Corresponding author email: israa78kirkuk@uokirkuk.edu.iq*

Received: 10 April 2026
Accepted: 05 June 2026
Published online: 12 June 2026

How to cite this article:

Sadiq IM, Nooruldeen SA. Distribution and variability of trabecular attenuation in the thoracic spine on routine chest CT. *Kirkuk Journal of Medical Sciences*. 2026;14(1):95–104.
DOI: 10.32894/kjms.2026.170731.1333

ABSTRACT

Background: Heterogeneity in vertebral trabecular bone attenuation may influence fracture risk. Chest computed tomography (CT) offers an opportunity to assess attenuation variability without additional radiation exposure. This study aimed to evaluate the distribution and variability of trabecular attenuation in the thoracic (T) vertebrae (T5–T12) on chest CT and to investigate the association between attenuation variability and chest wall composition.

Methods: This retrospective study included 101 adults aged 18–65 years who underwent chest CT. Trabecular attenuation was measured from T5 to T12, and attenuation variability was quantified using the coefficient of variation (CV%). Chest wall composition, including pectoralis major (PM) area and attenuation and subcutaneous fat area, was assessed at the T4 level. Associations were analyzed using Spearman correlation and multivariable linear regression.

Results: There was significant regional variation in thoracic vertebral trabecular characteristics. Mean trabecular attenuation progressively decreased from T5–T6 to T12 ($p < 0.001$), with relatively stable values across T7–T11. Attenuation variability was lowest at T5–T6, increased at T8–T9 ($p < 0.001$), and decreased again at T11–T12, with no significant difference between the two lowest segments ($p = 0.708$). On multivariable analysis, age was independently associated with increased attenuation variability ($B = 0.198$, $p < 0.001$). In contrast, PM muscle area ($p = 0.588$), PM muscle attenuation ($p = 0.080$), and subcutaneous fat area ($p = 0.263$) were not significantly associated with attenuation variability.

Conclusion: Thoracic vertebral trabecular attenuation and its variability show level-dependent variation. Age was significantly associated with increased attenuation variability, whereas sex and body composition parameters were not independent predictors.

Key words: Body composition; Computed tomography; Hounsfield units; Pectoralis major; Thoracic vertebrae.

ISSN: 2790-0207 (Print), 2790-0215 (Online).

INTRODUCTION

Vertebral trabecular bone in the thoracic spine plays a vital role in maintaining spinal stability [1]. Computed tomography (CT) is a reliable modality for assessing trabecular bone density, with attenuation values expressed in Hounsfield units (HU) serving as a surrogate marker of bone mineral content [2–5].

Recent advances in trabecular texture analysis and quantitative CT suggest that trabecular heterogeneity, quantified by coefficient of variation (CV) and spatial distribution patterns, may indicate architectural degradation. CV is an imaging measure that may provide information about bone quality and fracture risk, although it requires further clinical validation. Trabecular bone loss in osteoporosis is heterogeneous throughout the skeleton [6, 7]. Understanding trabecular microstructure may improve the evaluation and management of osteoporotic fractures and support surgical decision-making [1].

Body composition parameters, including skeletal muscle quality and adipose tissue distribution, influence bone health [8, 9]. Excess visceral and subcutaneous fat has been associated with variable effects on bone density [10, 11], whereas greater muscle mass and higher muscle quality are generally linked to improved bone strength [12–14].

Routine chest CT scans, increasingly performed for thoracic evaluation, offer an opportunity to assess thoracic vertebral bone quality without additional imaging or radiation exposure [15, 16]. Compared with the upper thoracic levels (T1–T4), the lower thoracic spine is less affected by beam-hardening artifacts caused by dense osseous structures of the shoulder girdle and upper limbs, which can degrade image quality [17]. Furthermore, previous studies have shown that muscle and fat measurements at the T4 level are strongly concordant with whole-body composition, supporting their use as a surrogate for L3-based assessments [18].

Many previous studies have focused on evaluating lumbar vertebrae using dedicated abdominal and lumbar CT protocols [19, 20]. In contrast, the regional distribution and variability of thoracic vertebral trabecular attenuation on routine chest CT remain insufficiently characterized. Although opportunistic CT has been widely applied for bone density assessment, limited data are available regarding trabecular attenuation variability and its relationship with regional chest body composition parameters.

Therefore, this study aimed to evaluate the distribution of trabecular bone attenuation, expressed in HU, and to assess attenuation variability using CV values across the mid- and lower-thoracic spine on routine chest CT scans. The study also investigated the association between trabecular attenuation variability and chest body composition parameters, including thoracic subcutaneous fat area, total PM muscle area, and mean PM attenuation measured at the T4 level.

MATERIALS AND METHODS

Study design

This retrospective cross-sectional study was conducted at a general teaching hospital between June 2024 and January 2026. Ethical approval was obtained from the local Ethics Committee of the College of Medicine, University of Kirkuk (Approval No. 80 B, dated 8 December 2025). The requirement for informed consent was waived because of the retrospective design. No financial support was provided, and patient-identifiable data were not accessed.

A total of 101 consecutive adult patients aged 18–65 years who underwent routine non-contrast chest CT examinations were included. The CT examinations were performed as part of the clinical evaluation of intrathoracic diseases. The inclusion criteria were age between 18 and 65 years, availability of non-contrast chest CT, and adequate image quality for quantitative analysis. The exclusion criteria were prior spinal surgery, vertebral fractures or tumors, CT images with significant motion or reconstruction artifacts, and age older than 65 years to reduce confounding from advanced degenerative changes. Information regarding osteoporosis, osteomalacia, hyperparathyroidism, corticosteroid use, osteoporosis treatment, biological therapy, and other metabolic bone conditions was not consistently available because of the retrospective design and therefore could not be incorporated into the analysis. Clinical indications for CT included evaluation of respiratory symptoms, infection, oncologic assessment, and follow-up of thoracic conditions. Because of the retrospective nature of the study, important clinical variables, such as body mass index (BMI), menopausal status, smoking history, steroid use, osteoporosis treatment, and chronic systemic diseases, were not available and were not included in the analysis.

Chest CT and quantitative analysis

All chest CT scans were performed using a 64-detector row scanner (Philips Healthcare). The acquisition parameters included automatic tube current modulation (DoseRight) with a tube voltage of 120 kVp. All images were reconstructed using a hybrid iterative reconstruction algorithm (iDose4, Philips) with a bone-specific kernel (Philips L, level 3) and a slice thickness of 4.0 mm. Examinations were performed with patients in the supine position while holding their breath during deep inspiration. Only non-contrast CT images were retrieved from the radiology system in DICOM format and analyzed using 3D Slicer software (version 5.7.1). All CT scans were reviewed and analyzed by a single radiologist with 15 years of experience in CT imaging.

Trabecular bone attenuation was measured in all vertebrae from T5 to T12 in every patient. For each vertebra, a single oval region of interest (ROI) was manually placed at the level of the pedicles within the central trabecular bone, carefully avoiding cortical bone, endplates, and the basivertebral vein [21]. The ROI size was kept as large as possible while remaining within the trabecular region. Attenuation values were recorded as mean ± standard deviation (HU). Trabecular attenuation variability was quantified using the coefficient of variation (CV). For each vertebral level, level-specific attenuation variability was calculated as the ROI standard deviation divided by the ROI mean attenuation and multiplied by 100. These level-specific CV values were used to describe attenuation variability from T5 to T12. In addition, an overall patient-level trabecular attenuation CV across T5–T12 was calculated and used for correlation and regression analyses. CV was calculated as follows:

$$\mathrm{CV} = \left(\frac{\mathrm{SD}}{\mathrm{mean}}\right) \times 100$$

where SD represents the standard deviation of attenuation values and the mean represents the average attenuation. CV reflects relative dispersion and serves as an indirect measure of trabecular heterogeneity [20].

Opportunistic body composition measurements were performed using a single axial slice at the T4 level. PM muscle area (cm^2) was measured using semi-automatic threshold segmentation of muscle tissue (−29 to 150 HU) with manual refinement of the bilateral PM muscles. Mean PM attenuation (HU) was also recorded to assess muscle quality. Measurements were taken from the right and left PM muscles. The mean of the two sides was used to analyze muscle attenuation, and the total area from both sides was used to analyze muscle area.

Subcutaneous fat area (cm^2) was segmented using semi-automatic thresholding of adipose tissue (−190 to −30 HU), excluding intrathoracic structures. Measurements included anterior, lateral, and posterior subcutaneous fat. Axillary and breast adipose tissue were included as part of the total subcutaneous fat area. Because breast tissue is present only in females and may influence fat measurements, sex-stratified analyses were performed to account for differences in fat distribution.

Statistical analysis

Jamovi software (version 2.5, 2024) was used for statistical analysis. Intra-observer reliability was evaluated by repeating the measurements in 13 randomly selected cases from the total sample of 101 patients after a three-week interval. The same radiologist, blinded to the initial results, performed the repeated measurements in a separate session. Reproducibility was evaluated using the intraclass correlation coefficient (ICC) and Bland–Altman analysis. ICC values were interpreted as poor (< 0.50), moderate (0.50–0.75), good (0.75–0.90), or excellent (> 0.90).

Normality was assessed using the Shapiro–Wilk test. Data were expressed as mean ± SD or median (interquartile range [IQR]), as appropriate. Group comparisons were performed using Student's *t*-test or the Mann–Whitney U test, as appropriate. Differences in mean trabecular attenuation and attenuation variability (CV) across vertebral levels (T5–T12) were evaluated using repeated-measures analysis of variance (ANOVA). Spearman correlation was used to assess associations between attenuation variability and body composition parameters. Multivariable linear regression analysis was performed to evaluate the independent predictors of trabecular attenuation variability. Coefficients (B), 95% confidence intervals (CIs), and *p*-values were reported. Multicollinearity was assessed using variance inflation factors (VIFs). A *p*-value of less than 0.05 was considered statistically significant.

RESULTS

Intra-observer reproducibility showed excellent agreement for all measurements. ICC values and Bland–Altman analysis results were as follows. For mean trabecular attenuation, Bland–Altman analysis demonstrated a mean difference of 0.75 HU between repeated measurements, with 95% limits of agreement ranging from −7.57 to 9.07 HU; intra-observer reliability was excellent (ICC = 0.91, 95% CI 0.82–0.98). For trabecular attenuation SD, the mean difference was 0.31 HU, with 95% limits of agreement ranging from −2.81 to 3.43 HU; intra-observer reliability was excellent (ICC = 0.94, 95% CI 0.83–0.98). For subcutaneous fat area, the mean difference was 50.55 cm^2, with 95% limits of agreement ranging from −127.93 to 229.03 cm^2; intra-observer reliability was excellent (ICC = 0.95, 95% CI 0.83–0.99). For PM muscle area, the mean difference was −1.10 cm^2, with 95% limits of agreement ranging from −8.01 to 5.80 cm^2; intra-observer reliability was excellent (ICC = 0.92, 95% CI 0.77–0.98). For PM muscle attenuation, the mean difference was −1.10 HU, with 95% limits of agreement ranging from −6.94 to 5.30 HU; intra-observer reliability was excellent (ICC = 0.94, 95% CI 0.83–0.98).

A total of 101 patients were included, with a balanced sex distribution. Baseline characteristics and morphometric data are summarized in Table 1. There was no significant age difference between males and females. However, significant sex-related differences were observed in body composition at the T4 level, with males demonstrating greater PM muscle area and higher PM attenuation, while females exhibited a higher subcutaneous fat area. No significant sex-based differ-

Table 1. Baseline characteristics, chest wall composition, and thoracic trabecular attenuation parameters of the study population.

Variable	Total (n = 101)	Male (n = 55)	Female (n = 46)	*p*-value
Demographic characteristic				
Age (years)	44.0 (35.0–55.0)	44.0 (35.0–52.0)	45.0 (35.0–56.8)	0.508
CT-derived chest wall composition at the T4 level				
Total pectoralis major muscle area (cm^2)	70.0 (49.9–91.5)	82.9 (67.8–116.8)	50.4 (41.7–64.0)	**<0.001**
Mean pectoralis major attenuation (HU)	35.2 (26.4–41.3)	40.5 (35.1–44.1)	25.9 (14.0–34.6)	**<0.001**
Subcutaneous fat area (cm^2)	528.8 (362.0–750.0)	383.0 (315.2–495.5)	761.5 (588.1–956.1)	**<0.001**
Thoracic trabecular attenuation parameters				
Mean trabecular attenuation (HU)	194.0 (158.8–212.0)	188.6 (167.6–207.6)	197.6 (99.9–262.0)	0.614
Trabecular attenuation SD (HU)	28.5 (25.1–32.0)	28.5 (18.2–51.8)	28.5 (25.6–31.3)	0.728
Trabecular attenuation CV (%)	16.0 (12.8–18.6)	16.0 (13.1–18.9)	15.5 (12.8–17.8)	0.738

Data are presented as median (interquartile range). Male and female groups were compared using the Mann–Whitney U test.
CT, computed tomography; CV, coefficient of variation; HU, Hounsfield units; SD, standard deviation.

Table 2. Thoracic vertebral trabecular attenuation and attenuation variability from T5 to T12.

Vertebral level	Trabecular attenuation Mean ± SD (HU)	Attenuation variability CV ± SD (%)
T5	196.13 ± 39.34	14.90 ± 5.48
T6	190.72 ± 40.70	15.67 ± 5.41
T7	185.44 ± 41.57	16.81 ± 6.03
T8	182.48 ± 42.36	17.66 ± 7.17
T9	184.38 ± 41.41	18.01 ± 7.16
T10	185.05 ± 43.99	17.58 ± 6.82
T11	182.57 ± 47.04	15.74 ± 6.24
T12	172.44 ± 47.89	15.16 ± 6.48

Data are presented as mean ± standard deviation for 101 cases. Repeated-measures ANOVA showed significant level-dependent variation in both trabecular attenuation and attenuation variability.
Level-specific CV values were calculated as the ROI standard deviation divided by the ROI mean attenuation at each vertebral level and multiplied by 100. These values describe attenuation variability at each vertebral level from T5 to T12.
ANOVA, analysis of variance; CV, coefficient of variation; HU, Hounsfield units; ROI, region of interest; SD, standard deviation.

ences were identified in trabecular attenuation parameters, including mean attenuation, SD, and CV.

Repeated-measures ANOVA established significant differences across thoracic vertebral levels (T5–T12) for both mean trabecular attenuation and CT-derived attenuation variability. Mauchly's test indicated violation of sphericity ($p < 0.001$); therefore, the Greenhouse–Geisser correction was applied for all analyses. Post hoc pairwise comparisons with Bonferroni adjustment demonstrated significant regional variation in trabecular attenuation and attenuation variability across the thoracic spine. Mean trabecular attenuation declined from the upper to the lower thoracic spine, with the highest values observed at T5 and T6 and the lowest at T12 ($p < 0.001$). Intermediate levels (T7–T11) showed relatively similar attenuation values without marked fluctuation. For trabecular attenuation variability (CV), post hoc comparisons showed that CV at T5–T6 was significantly lower than that at T8–T9 ($p < 0.001$). A subsequent reduction in variability was observed at the lower thoracic levels (T11–T12), with no significant difference between these final two segments ($p = 0.708$) (Table 2).

Spearman correlation analysis (Table 3) demonstrated significant inverse associations between mean vertebral trabecular CV and both total PM muscle area and mean PM attenuation. Specifically, a weak negative correlation was observed with total PM muscle area, whereas a moderate negative correlation was identified with mean PM attenuation. In contrast, no significant association was detected between subcutaneous fat area and trabecular bone CV in either sex.

Multiple linear regression analysis was performed to assess the extent to which the independent variables predicted trabecular bone CV. The model showed moderate explanatory power, accounting for 33.4% of the variance in the outcome ($R^2 = 0.334$). Model assumptions and overall model fit were evaluated using standard diagnostic procedures. Residual normality was assessed using the Shapiro–Wilk test, which indicated a statistically significant deviation from normality ($p < 0.001$). However, visual inspection of the Q–Q plot showed that the residuals were approximately normally distributed, with only minor deviations in the upper tail. Homoscedasticity and linearity were examined using residual

Table 3. Spearman correlation between trabecular attenuation variability and CT-derived body composition parameters.

Body composition parameter	Spearman correlation coefficient (r_s)	*p*-value
Total pectoralis major muscle area (cm^2)	−0.199	**0.046**
Mean pectoralis major attenuation (HU)	−0.262	**0.008**
Subcutaneous fat area in males (cm^2)	−0.154	0.262
Subcutaneous fat area in females (cm^2)	0.071	0.639

The outcome variable was trabecular attenuation variability, expressed as the coefficient of variation.
CT, computed tomography; HU, Hounsfield units; r_s, Spearman rank-order correlation coefficient.

Table 4. Multivariable linear regression analysis of factors associated with trabecular attenuation variability.

Predictor variable	B coefficient	95% CI	*p*-value
Age (years)	0.198	0.122, 0.273	**<0.001**
Total pectoralis major muscle area (cm^2)	−0.009	−0.042, 0.024	0.588
Mean pectoralis major attenuation (HU)	−0.109	−0.232, 0.013	0.080
Subcutaneous fat area (cm^2)	−0.003	−0.008, 0.002	0.263
Sex (male–female)	2.002	−0.680, 4.684	0.142

The dependent variable was trabecular attenuation variability, expressed as the coefficient of variation.
B, unstandardized regression coefficient; CI, confidence interval; HU, Hounsfield units.

plots, which revealed no substantial violations. Influential observations were assessed using Cook's distance, with a maximum value of 0.224, indicating no influential outliers. Multicollinearity among predictors was evaluated using VIFs, which ranged from 1.27 to 2.73 and suggested no evidence of multicollinearity. Overall model fit was assessed using the coefficient of determination (R^2 = 0.334). A two-sided significance level of $p < 0.05$ was adopted for all statistical analyses. As shown in Table 4, age was positively related to trabecular bone CV and was the only statistically significant independent variable. Other variables, including total PM area, PM muscle attenuation, subcutaneous fat area, and sex, were not significant predictors of trabecular bone CV after adjustment. To account for sexual dimorphism in fat distribution, sex was included as a covariate in the multivariable model, allowing assessment of the impact of subcutaneous fat independent of sex-specific baseline differences.

Linear regression analysis was conducted to assess the relationship between trabecular bone CV and patient age. The scatter plot shown in Figure 1 demonstrated a statistically significant positive linear correlation, suggesting that increasing age was associated with increasing trabecular bone CV. The regression line showed a steady upward trend across the age range of approximately 18–65 years, with most data points distributed around the fitted regression line. Although the trend was consistent in younger and middle-aged patients, greater data scatter and outliers were observed in patients older than 60 years, indicating greater variability in bone composition in later life.

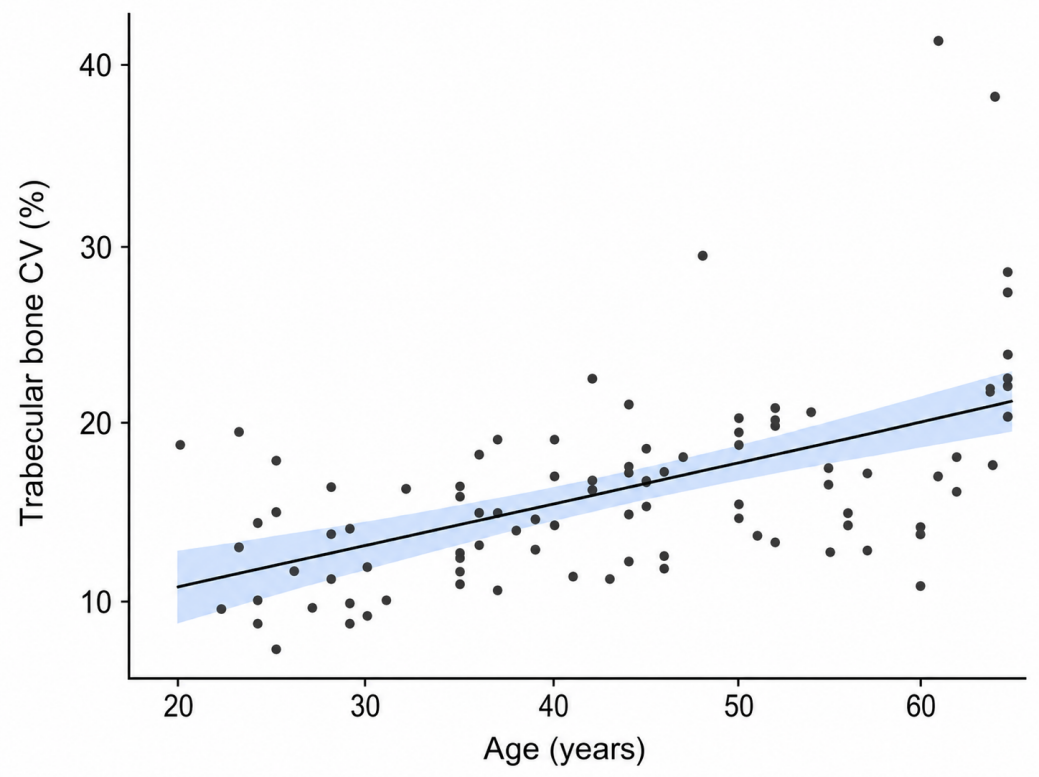

Figure 1. Scatter plot demonstrating the linear relationship between age (years) and trabecular bone CV (%). The solid line shows the linear regression trend, and the shaded area shows the 95% confidence interval.

DISCUSSION

In this study, there was no significant difference in mid- and lower-thoracic vertebral trabecular attenuation or attenuation variability between male and female groups. Similarly, sex was not identified as an independent predictor in the multivariable regression analysis. Previous studies have shown no considerable sex-related differences in vertebral cancellous bone strength, bone volume fraction, or trabecular density and attenuation variability [20, 22, 23]. However, other studies found significant sex-related differences only in certain age groups and at certain spinal sites [24, 25]. These observations suggest that factors such as aging and anatomy may influence vertebral trabecular characteristics more than sex does.

The present analysis demonstrated a decline in mean trabecular attenuation from T5 to T12, with the highest values observed at T5 and T6 and the lowest at T12. This finding is consistent with several previous studies [26–28].

In contrast, attenuation variability (CV) followed a different pattern, increasing from T5 to peak at T8–T9 before declining toward T11–T12. This divergence between mean attenuation and variability may reflect the biomechanical properties of the thoracic spine. The rib cage stabilizes the upper and mid-thoracic spine; therefore, trabecular attenuation at these levels may be more homogeneous. At the T8–T9 levels, the stabilizing forces of the rib cage may decrease, potentially contributing to stress-related attenuation changes and increased variability. Meanwhile, at the lower thoracic levels, loading becomes predominantly axial and more uniform, which may explain the reduction in trabecular attenuation variability observed at T11–T12. These findings suggest that regional thoracic spine biomechanics and loading forces may influence trabecular attenuation variability [29, 30].

Beyond these biomechanical factors, the non-linear pattern may be influenced by several physiological and technical variables. Regional variations in vertebral marrow composition, particularly the transition from red to yellow marrow, can affect bone attenuation heterogeneity. In addition, progressive changes in thoracic kyphosis, combined with variations in vertebral size and shape, may influence local load transmission and the spatial distribution of bone density. Finally, the proximity of these levels to the diaphragm introduces the potential for respiratory motion artifacts, which may disproportionately affect measurements at specific thoracic segments. Consequently, trabecular attenuation variability is likely influenced by a complex interplay of regional biomechanics, marrow composition, and technical imaging constraints [31–33].

The present study found that vertebral trabecular attenuation variability increased with advancing age. This finding is consistent with many previous studies that identified age as a key factor associated with reduced bone homogeneity. With aging, the bone-remodeling process becomes imbalanced, with osteoclastic bone resorption exceeding osteoblastic bone

formation. This imbalance may result in trabecular perforation, thinning, and loss of connectivity, processes that can affect trabecular attenuation homogeneity [34].

In univariate analysis, total PM muscle area and mean PM attenuation showed significant inverse correlations with trabecular attenuation variability. However, these parameters were not independent predictors after adjustment in the multivariable regression model. This suggests that their association with vertebral attenuation variability may be partly explained by age, sex, or other covariates. Local mechanical loading may play a more important role in the muscle–bone relationship than systemic effects alone. The PM muscle primarily contributes to upper limb movement and has limited direct biomechanical interaction with the thoracic vertebrae. In contrast, the paraspinal muscles are functionally and anatomically linked to the spine and contribute directly to spinal stability and load transmission. Consequently, paraspinal muscle quality may demonstrate a stronger association with vertebral bone characteristics than chest wall musculature [35, 36]. Moreover, subcutaneous fat is a peripheral fat depot and may have less metabolic interaction with bone than visceral fat. This finding is consistent with several studies [37]. Increased attenuation variability may reflect age-related alterations in trabecular structure and could potentially provide complementary information regarding bone quality beyond mean attenuation alone. However, the clinical significance of this metric remains uncertain and requires validation against established reference standards, including dual-energy X-ray absorptiometry (DXA), quantitative CT, and longitudinal fracture outcomes, before it can be considered for clinical risk stratification.

The present study has several limitations, including the potential for selection bias and its single-center design. The use of a single-level body composition measurement is another limitation. In addition, the use of routine chest CT with a section thickness of 4 mm may limit the precision and interpretation of the biological significance of CV. Because of the retrospective design, potentially important confounding clinical variables, such as BMI and diseases affecting bone health, were not available. Furthermore, attenuation variability was not validated against DXA-derived bone mineral density, dedicated quantitative CT measurements, or incident fracture outcomes. Therefore, the clinical utility of this parameter as a biomarker of bone quality or fracture susceptibility remains to be established. Although inter-observer variability is important for generalizability, the primary aim of this study was to investigate biological variability in trabecular attenuation rather than measurement variability. Standardized ROI placement and consistent analysis by a single experienced observer were used to minimize technical variation.

CONCLUSION

Routine chest CT may provide useful opportunistic information about vertebral bone characteristics. However, the clinical relevance of attenuation variability requires further validation against established measures of bone density, bone microarchitecture, and fracture risk before routine clinical implementation. Vertebral trabecular attenuation and its variability exhibit distinct regional patterns along the thoracic spine, which may reflect underlying biomechanical and anatomical influences. While mean attenuation decreases progressively from the upper to lower thoracic levels, attenuation variability demonstrates a non-linear distribution, peaking in the mid-thoracic region. Among the included factors, age emerged as the only significant factor associated with increased trabecular attenuation variability.

ETHICAL DECLARATIONS

- **Ethics Approval and Consent to Participate**

  Ethical approval was obtained from the local Ethics Committee of the College of Medicine, University of Kirkuk (Approval No. 80 B, dated 8 December 2025). The requirement for informed consent was waived because of the retrospective nature of the study. Patient-identifiable data were not accessed.

- **Consent for Publication**

  Not applicable.

- **Availability of Data and Material**

  The datasets generated and analyzed during the current study are available from the corresponding author upon reasonable request.

- **Competing Interests**

  The authors declare that they have no competing interests, financial or otherwise, that could be perceived as influencing the work reported in this manuscript.

- **Funding**

  This research received no specific grant from any funding agency in the public, commercial, or not-for-profit sectors.

- **Use of Generative Artificial Intelligence**

The authors declare that ChatGPT, a generative AI-based tool developed by OpenAI, was used solely to enhance clarity and grammatical accuracy during the final editing phase. It was not used for content generation, data analysis, or interpretation.

- **Authors' Contributions**

All authors contributed equally to the study conception and design. All authors reviewed the manuscript and approved the final manuscript.

REFERENCES

[1] Schröder G, Mittlmeier T, Gahr P, Ulusoy S, Hiepe L, Schulze M, et al., Regional variations in the intra-and intervertebral trabecular microarchitecture of the osteoporotic axial skeleton with reference to the direction of puncture. *Diagnostics* 2024;14(5):498. https://doi.org/10.3390/diagnostics14050498

[2] Marques ML, Pereira da Silva N, van der Heijde D, Reijnierse M, Baraliakos X, Braun J, et al., Hounsfield Units measured in low dose CT reliably assess vertebral trabecular bone density changes over two years in axial spondyloarthritis. *Seminars in Arthritis and Rheumatism* 2023;58:152144. https://doi.org/10.1016/j.semarthrit.2022.152144

[3] Alharthy A, Assessment of trabecular bone Hounsfield units in the lumbar spine for osteoporosis evaluation in individuals aged 65 and above: a review. *Osteoporosis International* 2025;36:225–233. https://doi.org/10.1007/s00198-024-07340-w

[4] Buenger F, Sakr Y, Eckardt N, Senft C, Schwarz F, Correlation of quantitative computed tomography derived bone density values with Hounsfield units of a contrast medium computed tomography in thoracolumbar vertebral bodies. *Archives of Orthopaedic and Trauma Surgery* 2022;142:3335–3340. https://doi.org/10.1007/s00402-021-04184-5

[5] Yaprak G, Gemici C, Seseogullari OO, Karabag IS, Cini N, CT-derived Hounsfield unit: an easy way to determine osteoporosis and radiation-related fracture risk in irradiated patients. *Frontiers in Oncology* 2020;10:742. https://doi.org/10.3389/fonc.2020.00742

[6] Chia KK, Haron J, Nik Malek NFS, Accuracy of computed tomography attenuation value of lumbar vertebra to assess bone mineral density. *Malaysian Journal of Medical Sciences* 2021;28(1):41–50. https://doi.org/10.21315/mjms2021.28.1.6

[7] Andresen JR, Schröder G, Haider T, Andresen R, Opportunistic Osteoporosis Assessment and Fracture Risk Determination Using Cancellous Density Measurement in Hounsfield Units of Native Lumbar Computed Tomography Images—A Comparative Study with Conventional Bone Density Evaluation. *Journal of Clinical Medicine* 2025;14(4):1226. https://doi.org/10.3390/jcm14041226

[8] Yanmeng Q, Han Y, Dandan L, Xiao W, Xitong J, Xuesong S, Association between body composition components and bone mineral density in older adults. *Scientific Reports* 2025;15(1):26190. https://doi.org/10.1038/s41598-025-11642-2

[9] Spanoudaki M, Giaginis C, Mentzelou M, Bisbinas A, Solovos E, Papadopoulos K, et al., Sarcopenia and sarcopenic obesity and osteoarthritis: A discussion among muscles, fat, bones, and aging. *Life* 2023;13(6):1242. https://doi.org/10.3390/life13061242

[10] Lin Y, Zhong X, Lu D, Yao W, Zhou J, Wu R, et al., Association of visceral and subcutaneous fat with bone mineral density in US adults: a cross-sectional study. *Scientific Reports* 2023;13(1):10682. https://doi.org/10.1038/s41598-023-37892-6

[11] Sharma DK, Anderson PH, Morris HA, Clifton PM, Visceral fat is a negative determinant of bone health in obese postmenopausal women. *International Journal of Environmental Research and Public Health* 2020;17(11):3996. https://doi.org/10.3390/ijerph17113996

[12] Walowski CO, Herpich C, Enderle J, Koch M, Stelmach-Mardas M, Vickery C, et al., Determinants of bone mass in older adults with normal- and overweight derived from the crosstalk with muscle and adipose tissue. *Scientific Reports* 2023;13:5030. https://doi.org/10.1038/s41598-023-31642-4

[13] Riviati N, Darma S, Reagan M, Iman MB, Syafira F, Indra B, Relationship between muscle mass and muscle strength with bone density in older adults: a systematic review. *Annals of Geriatric Medicine and Research* 2025;29(1):1–14. https://doi.org/10.4235/agmr.24.0113

[14] Qin H, Jiao W, Correlation of muscle mass and bone mineral density in the NHANES US general population 2017–2018. *Medicine (Baltimore)* 2022;101(39):e30735. https://doi.org/10.1097/MD.0000000000030735

[15] Thuere KL, Mantz L, Sultana S, Henderson LM, Sakoda LC, Kazerooni E, et al., Opportunistic screening on chest CT, from the AJR special series on screening. *American Journal of Roentgenology* 2026;226(4):e2533069. https://doi.org/10.2214/AJR.25.33069

[16] Yang J, Liao M, Wang Y, Chen L, He L, Ji Y, et al., Opportunistic osteoporosis screening using chest CT with artificial intelligence. *Osteoporosis International* 2022;33(12):2547–2561. https://doi.org/10.1007/s00198-022-06491-y

[17] Kane AG, Reilly KC, Murphy TF, Swimmer's CT: improved imaging of the lower neck and thoracic inlet. *AJNR American Journal of Neuroradiology* 2004;25(5):859–862. https://pubmed.ncbi.nlm.nih.gov/15140736/

[18] Daly A, Newman L, Thomas A, Munro A, Spence C, Long J, et al., Assessment of body composition in breast cancer patients: concordance between transverse computed tomography analysis at the fourth thoracic and third lumbar vertebrae. *Frontiers in Nutrition* 2024;11:1366768. https://doi.org/10.3389/fnut.2024.1366768

[19] Cheng X, Zhao K, Zha X, Du X, Li Y, Chen S, et al., Opportunistic screening using low-dose CT and the prevalence of osteoporosis in China: a nationwide multicenter study. *Journal of Bone and Mineral Research* 2021;36(3):427–435. https://doi.org/10.1002/jbmr.4187

[20] Cai J, Chen L, Liu L, Yi J, Wu J, Yang T, et al., Regional variations and spatial heterogeneity of lumbar CT attenuation are associated with osteoporotic vertebral fracture. *Frontiers in Endocrinology (Lausanne)* 2025;16:1630371. https://doi.org/10.3389/fendo.2025.1630371

[21] Yajima T, Kurisawa A, Arao M, Computed tomography-measured trabecular attenuation at first lumbar vertebra as a surrogate marker of bone mineral density and osteoporosis in patients undergoing hemodialysis. *Renal Failure* 2026;48(1). https://doi.org/10.1080/0886022X.2026.2671455

[22] Lochmüller EM, Pöschl K, Würstlin L, Matsuura M, Müller R, Link TM, et al., Does thoracic or lumbar spine bone architecture predict vertebral failure strength more accurately than density? *Osteoporosis International* 2008;19(4):537–545. https://doi.org/10.1007/s00198-007-0478-x

[23] Samelson EJ, Christiansen BA, Demissie S, Broe KE, Louie-Gao Q, Cupples LA, et al., QCT measures of bone strength at the thoracic and lumbar spine: The Framingham study. *Journal of Bone and Mineral Research* 2012;27(3):654–663. https://doi.org/10.1002/jbmr.1482

[24] Simion G, Eckardt N, Ullrich BW, Senft C, Schwarz F, Bone density of the cervical, thoracic and lumbar spine measured using Hounsfield units of computed tomography–results of 4350 vertebras. *BMC Musculoskeletal Disorders* 2024;25:200. https://doi.org/10.1186/s12891-024-07324-1

[25] Otsuka H, Tabata H, Ito N, Shi H, Iwashimizu T, Kaga H, et al., Age-related differences in bone structural parameters using 3D-DXA and TBS in men and women: The Bunkyo Health Study. *Bone* 2025;199:117549. https://doi.org/10.1016/j.bone.2025.117549

[26] Lee M, Lee E, Lee JW, Value of computed tomography Hounsfield units in predicting pedicle screw loosening in the thoracic spine. *Scientific Reports* 2022;12(1):18279. https://doi.org/10.1038/s41598-022-23142-8

[27] Salzmann SN, Okano I, Jones C, Basile E, Iuso A, Zhu J, et al., Thoracic bone mineral density measured by quantitative computed tomography in patients undergoing spine surgery. *The Spine Journal* 2021;21(11):1866–1872. https://doi.org/10.1016/j.spinee.2021.05.016

[28] Yang Y, Liao F, Xing X, Liao N, Wang D, Yin X, et al., The reduced cortical bone density in vertebral bodies: risk for osteoporotic fractures? Insights from CT analysis. *Journal of Orthopaedic Surgery and Research* 2024;19(1):486. https://doi.org/10.1186/s13018-024-04896-5

[29] Schröder G, Reichel M, Spiegel S, Schulze M, Götz A, Bugaichuk S, et al., Breaking strength and bone microarchitecture in osteoporosis: a biomechanical approximation based on load tests in 104 human vertebrae from the cervical, thoracic, and lumbar spines of 13 body donors. *Journal of Orthopaedic Surgery and Research* 2022;17(1):228. https://doi.org/10.1186/s13018-022-03105-5

[30] Liebsch C, Wilke HJ, How Does the Rib Cage Affect the Biomechanical Properties of the Thoracic Spine? A Systematic Literature Review. *Frontiers in Bioengineering and Biotechnology* 2022;10:904539. https://doi.org/10.3389/fbioe.2022.904539

[31] Cheng X, Li K, Zhang Y, Wang L, Xu L, Liu Y, et al., The accurate relationship between spine bone density and bone marrow in humans. *Bone* 2020;134:115312. https://doi.org/10.1016/j.bone.2020.115312

[32] Pavlovic A, Nichols DL, Sanborn CF, Dimarco N, Relationship of thoracic kyphosis and lumbar lordosis to bone mineral density in women. *Osteoporosis International* 2013;24(8):2269–2273. https://doi.org/10.1007/s00198-013-2296-7

[33] Kim D, Choi J, Lee D, Kim H, Jung J, Cho M, et al., Motion correction for routine X-ray lung CT imaging. *Scientific Reports* 2021;11(1):3695. https://doi.org/10.1038/s41598-021-83403-w

[34] Chan CH, Wu HY, Chen LH, Vu Pham Thao V, Liang CH, Ting YW, et al., Vertebral trabecular microarchitecture changes in the normally ageing population. *Quantitative Imaging in Medicine and Surgery* 2026;16(1):79. https://doi.org/10.21037/qims-2025-1453

[35] Smith C, Sim M, Dalla Via J, Levinger I, Duque G, The interconnection between muscle and bone: A common clinical management pathway. *Calcified Tissue International* 2024;114:24–37. https://doi.org/10.1007/s00223-023-01146-4

[36] Ozer FF, Güler E, Relation of bone mineral density with fat infiltration of paraspinal muscles: the Goutallier classification. *Osteoporosis and sarcopenia* 2024;10(2):84–88. https://doi.org/10.1016/j.afos.2024.04.002

[37] Vári B, Győri F, Katona Z, Berki T, The impact of age and body composition on bone density among office worker women in Hungary. *International journal of environmental research and public health* 2023;20(11):5976. https://doi.org/10.3390/ijerph20115976